Research Article

Journal of RAMAN SPECTROSCOPY

Received: 5 September 2011 Revised: 14 October 2011 Accepted: 28 October 2011 Published online in Wiley Online Library: 23 May 2012

(wileyonlinelibrary.com) DOI 10.1002/jrs.3123

Origin of the variability of the mechanical properties of silk fibres: 2 The nanomechanics of single silkworm and spider fibres

Philippe Colomban* and Hung Manh Dinh

The variability in mechanical stress–strain behaviour of various silks obtained from *Bombyx mori* silkworm and *Nephila madagascarensis* spider fibres has been studied by high resolution Raman analysis using the Raman shift induced by application of a controlled strain on the νN–H mode as a probe. Silk fibres exhibiting typical 1, 2, 3 and 4 Types have been selected from their characteristic tensile stress–strain behaviour. A perfect relationship between the nanomechanic (at the scale of the chemical bond) and macroscopic (silk single fibre) behaviour is observed as in the case of other polyamide fibres (natural keratin and synthetic PA66). Copyright © 2012 John Wiley & Sons, Ltd.

Supporting information may be found in the online version of this article.

Keywords: fibres; silk; *Bombyx mori*; spider; mechanics

Introduction

Silkworm silk has been a commodity for over 3000 years. Its use is explained by an exceptional combination of mechanical properties and thermal stability. Its biodegradability and biocompatibility offer many opportunities for new applications (drug delivery, artificial membranes).[1–5] Variability of mechanical properties of natural fibres limits their use, even though the inevitable inflation of petroleum-based synthetic products creates an incentive to use natural or biosourced products. Therefore, alongside the efforts of genetic selection and modification and the control of producing silk, a better understanding of the variability and its origins is required.

The study of the Raman shift induced by the application of a controlled tensile load or strain on a single fibre gives information about the material conformation/structure changes.[6–14] However, the anharmonicity of the bond potential means that external perturbations (temperature, pressure, stress) lead to a wavenumber shift that depends on the bond anharmonicity, the bond length change, the structure and orientation of the bond.[15] The lengthening limit of most chemical bonds is small (< 2–3%), the wavenumber shift remains small, a few % at best before failure, and highly depends on the bond anharmonicity. Resonance Raman spectroscopy offers the multiplication of sensitivity by two (1st harmonic) or three times (2nd harmonic) when their intensity is sufficient. Such cases are very rare and actually effective for carbon fibres.[15,16] Another possibility to obtain significant Raman shifts is by considering very anharmonic modes such as those involved in hydrogen-bonded species.

In a previous work[13] the tensile load-induced Raman shift of the low-range and medium-range wavenumber modes has been studied for degummed *Bombyx mori* single fibres. This study pointed out the change of behaviour at ~3% of applied strain, the limit of the Hookean regime. The very collective modes below 200 cm^{-1}, as observed for many semi-crystalline fibres[7,8,12] show the largest wavenumber shifts. These modes are highly polarised because of the high orientation of the *B. mori* macromolecules of fibroin along the fibre axis.[13] Because of the strong overlapping of peaks, with the Rayleigh wing, the determination of the component' centre of gravity is not very accurate.

The extensive analysis of the stress–strain behaviour of series of (silkworms, spider) silk fibres[17–19] has demonstrated that five different behaviour types can be observed (Fig. 1). These types are directly correlated to the degree of crystallinity, water content, degradation and sample history (age, drying, dyeing ...). The molecular backbone of silk proteins (fibroin and spidroin) consists of a polyamide chain, built of four groups of atoms: three groups form the amine one, the last R group, the so-called aminoacid residue (because they form aminoacids after breaking/hydrolysis of the chain) varies in size, charge, hydrogen bonding capacity and chemical reactivity. About 20 different R groups are observed, the most frequent being glycine, alanine and serine (glutamic acid) for silkworm (spider) fibres.[5,13] The latter R-groups are small in size permitting a decrease of the interchain distance and hence higher density and mechanical properties. In this paper, we will compare the nanomechanics of the different silk fibres exhibiting the various stress–strain behaviours using the main ν N–H mode because of the huge sensitivity of this very anharmonic bond to probe modification of the local structure, as previously shown for synthetic polyamide fibres.[6,7,12,15]

* *Correspondence to: Philippe Colomban, Laboratoire de Dynamique, Interactions et Réactivité, UMR 7075 CNRS, Université Pierre et Marie Curie-Paris 6, 4 Place Jussieu, c49, 75252 Paris Cedex 05, France. E-mail: philippe.colomban@upmc.fr*

Laboratoire de Dynamique, Interactions et Réactivité, UMR 7075 CNRS, Université Pierre et Marie Curie-Paris 6, 4 Place Jussieu, c49, 75252 Paris Cedex 05, France

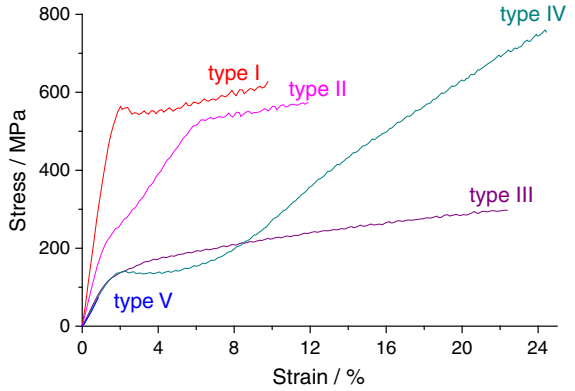

Figure 1. The five types of stress–strain curve of natural silk fibres. The Type V curve superimposes with types IV and V; the fracture takes place at 2–4% of strain, typically. See Refs [17,18,20] for details.

Material and methods

Materials

The materials studied have been extensively described in the previous paper.[19] A series of domestic *B. mori* silk fibres have been extracted from: (i) hand-spun silkworm bave at the moment when it started to make its cocoon (fresh undegummed fibre); (ii) fresh or aged (days to year) cocoons produced at INRA (Institut National de la Recherche Agronomique, Unité Sériciole Nationale, La Mulatière, France) or at another experimental farm in Tunisia; (iii) degummed and gummed flotte and cocoon; and (iv) *Nephila madagascarensis* (*Nm*) single fibres extracted from a ~20-cm long bundle. Note that the spider fibre was free from any sericine coating although a sericine sheath coats the undegummed silkworm bave, actually made of two adjacent fibres. The spider fibres date from the 1990s when a private silk production was created in Madagascar with USN-INRA collaboration. The extracted bave/fibre was first cut into ~100-mm-long samples and then cut again in three parts, which were mounted and stuck on a paper frame as previously described.[6–8,13] It was mandatory that no stress was applied to the fibre during the mounting–sticking procedure. Fibres were stored and handled at ~60% relative humidity. Some fibres were saturated with water by immersion for at least 2 days in water and/or dried at 105 °C.[6,8,17,20]

Methods

The mechanical tensile properties of the samples were obtained using a computer controlled DISCAPELEC Universal Fibre Tester (UFT). The gauge length was 30 mm (see Refs [18–20] for details). The Tester was set under the ×50 long working distance objective (numerical aperture: 0.45, total magnification ×500, OLYMPUS, Japan) of a high resolution XY Raman spectrometer (Dilor, France (Fig. 2)) equipped with a N_2-cooled charge-coupled device detector. The orientation of the tester versus the laser polarisation was chosen to obtain the stronger N-H signal.[13]

Selection of the samples were made using a Labram Infinity (Notch filtered, Peltier cooled high sensitivity instrument) using 532 nm YAG laser illumination.

Measurements at different temperatures were made using an Air Liquide (Sassenage, France) Helium cooled cryostat and a HR 800 Labram Horiba Jobin Yvon (Longjumeau, France) instrument under 514.5 nm illumination.

All Raman measurements were performed with the same procedure: the recording time equal to 1800 or 3600 s was repeated 4 to 12 accumulations to wisp out the cosmic peaks and to obtain spectra having a good signal-to-noise ratio under 2 mW 514.5 nm illumination. Fibres were studied at the different stress levels up to their failure. After failure, spectra were recorded at the fracture tip of the broken fibre. As described in a previous paper, the wavenumber position was controlled using a neon lamp.[13] Actually, all spectra were in the right position relative to the neon peaks and there was no need for position correction. The spectra of degummed Bm fibres were free from background noise and no baseline subtraction was needed. The LABSPEC software (Dilor) was used for subtracting the background signal of spider silk spectra.

The band component analysis was performed using ORIGIN 5.0 software (Microcal, USA).[6,8] As previously described,[6–10,13] the following assumptions were made: a Lorentz shape was chosen for the narrow and/or symmetric peak characteristic for ordered material.[21] Broad components characteristic of amorphous material or vibrators with a large static or dynamic disorder were fitted using a Gaussian curve.

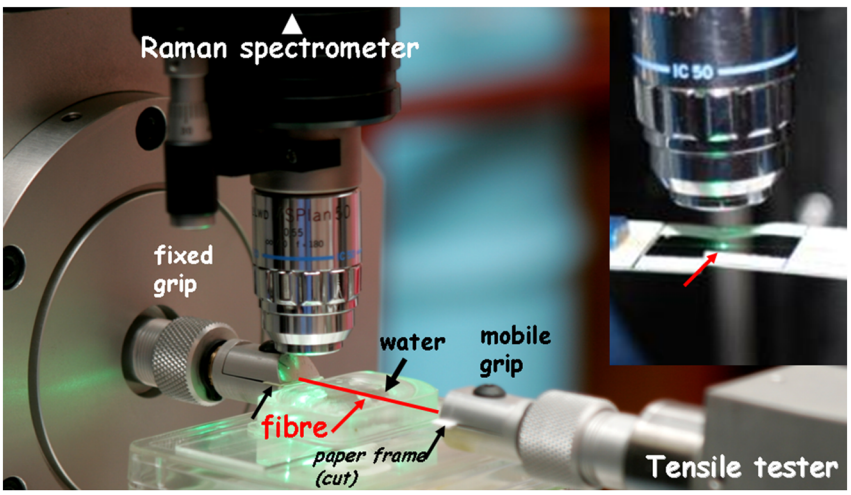

Figure 2. Detail of the Raman set-up for measurement of single fibre under controlled load or strain, for a water saturated fibre (the paper frame has been cut close to the grips and the fibre is put in contact with the water meniscus in between recording sequences); the insert shows the laser focussed on the fibre.

Journal of RAMAN SPECTROSCOPY

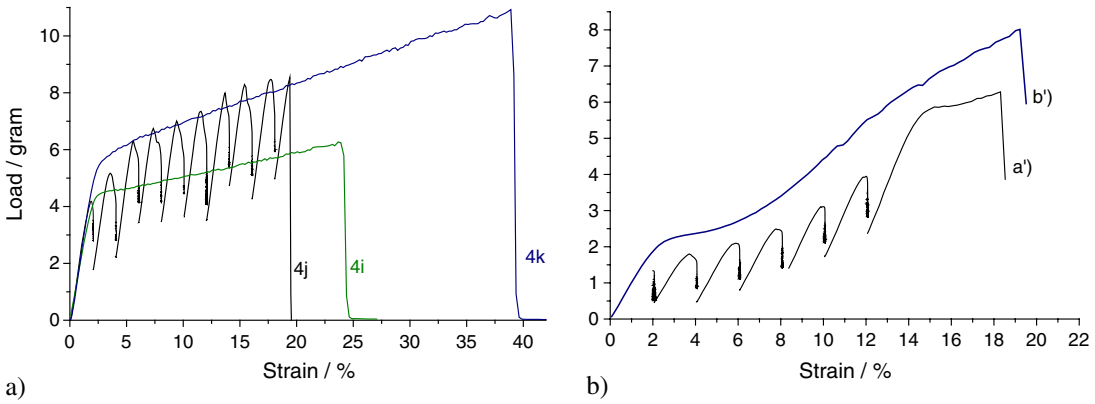

Figure 3. (a) Type I behaviour of a very fresh *Bm* silk fibre that was used for the Raman analysis under controlled strain. The samples 4i and 4 k are adjoining samples prepared from the same fibre. The 4i and 4 k pieces of fibre are Type I, so the selected 4j one can be considered of Type I. The plot of the 4j sample was recorded during the Raman experiment, a partial unload–load event was made after each recorded spectrum at a level of strain; (b) Type IV behaviour of a dried *Nephila* fibre used for the measurement. The b'-sample is adjoining the Raman studied a'-sample; the plot was recorded during the Raman experiment, each partial unload–load cycle being made after the recording of the spectrum.

To be sure that the fibre selected because of preparation criteria (hand stressed fresh *Bm* fibre for Type I, freshly obtained from a *Bm* cocoon for type II, water saturated degummed *Bm* fibre for type III and dried *Nephila* fibre for type IV) was of the expected type, a series of samples were prepared from the same fibre length, named by the letter of the alphabet (a, b, c, . . ., Fig. 3). The first sample (a) and the last one (e.g. d) were tested in tension. If the expected type behaviour was obtained for the two a and d samples, the sample b and c could be considered as those having the same type behaviour. About 20 selected *Bm* fibres were carefully identified with different types. Furthermore, partial unloading/loading cycles could be made before the fibre breaks in between recording sequence to control the stress–strain behaviour (Figs. 3a (4i, 4j & 4k lines) & 3b (a' line)).

Results and discussion

Figure 1 shows representative examples of the five different types of signatures that could be identified. For each series, whatever the creature, different stress *versus* strain curves could be distinguished:

- Type I exhibits linear elastic behaviour up to 2% of strain and then a quasi plateau is observed;
- Type II consists of two-step linear elastic behaviours up to 5–6% with kinks at ~2 and 5–6%, and then shows a quasi plateau.
- Type III is characterized by a smooth transition from a linear behaviour to a plateau.
- Type IV starts rather similar to that of type I but above ~8–12% a quasi-linear 2nd behaviour is observed, rather similar to the hardening observed for many metallic materials.
- Type V: the fibres break during the first elastic stage.

Type IV is observed for sericine-free, dried or old fibres. Type III is characteristic for fibres saturated with water. Type I is observed for fresh spun, sericine coated fibres (baves). Type II is more frequent for fibres extracted from textile gummed yarns. Type V behaviour is only detected for heavy chemically (acid/base or dyed degummed fibres) or thermally treated samples, i.e. after some degradation.

The νN–H Raman probe

Figure 4 shows room temperature (RT) and helium temperature spectra of *Bm* degummed fibre with details for the νN–H region (also called amide A). The main difference consists in the narrowing and bathochromic shift (~3465 to 3425 cm^{-1}) of the main

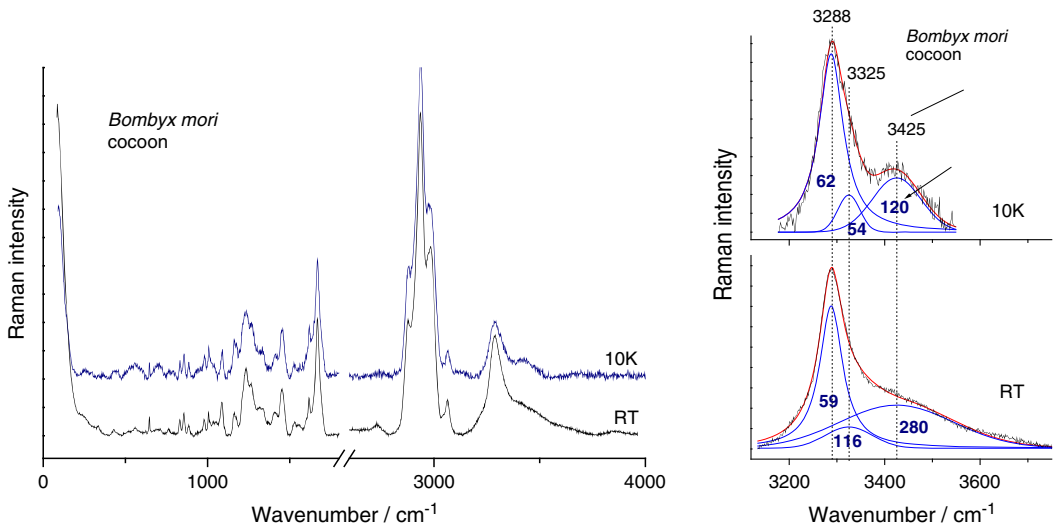

Figure 4. Comparison of the Raman spectra recorded at room and at helium (10 K) temperature of Type IV fibre (drying is due to the low temperature and vacuum).

board component, a Gaussian band previously observed in different silks, keratin and synthethic polyamide fibres[6–8] and assigned to water molecule on the basis of deuteration and water content.[9] The ~60 cm^{-1} bandwidth of the 3284 cm^{-1} Lorentzian component at RT (3288 cm^{-1} at 10 K) assigned to the N–H vibrators in well defined ('crystalline') polymer remains unchanged, which shows a stable environment. The latter band will be used as a nanomechanical probe. By comparison the corresponding bandwidth measured for synthetic PA66 semi-crystalline polyamide at RT is equal to 20 cm^{-1}.[6–10] This confirms the low crystallinity of the 'ordered' silk. The small third component detected at ~3325 cm^{-1} has been assigned to N–H vibrators in highly disordered regions. Its narrowing from 116 to 54 cm^{-1}, i.e. a value similar to that of the main N–H band, may indicate a dynamic disorder of N–H vibrators in disordered, amorphous regions. The bandwidth measured at helium temperature in silk corresponds to that measured for N–H vibrators (at room temperature) in PA66.[9] It can be expected that the lower density of bands/unit volume in amorphous zones facilitates the high dynamic disorder. The higher wavenumber measured for 'amorphous' N–H vibrators is also consistent with larger distances between H and neighbouring acceptors. It has been pointed out that 'amorphous' chains play a prominent role in the fatigue and failure behaviour of PA66 fibres[7,24] and similar behaviour may be expected for silk fibres. The study of the amorphous component would be very informative. However, because of its low intensity and complete overlapping with other components the reliability of the conclusion may be poor.

The N–H signature of *N. madagascarensis* is more complex: two components with rather similar intensities are observed at ~3224 and 3283 cm^{-1}.[13] The latter, stronger one will be used as a nanomechanical probe. These very different N–H signatures indicate the more complex structure of spider silk. A band at ~3395 cm^{-1}, assigned to water is also observed. The hydrogen bonding with a wavenumber close to 3285 cm^{-1} is almost ineffective.

The νN–H (y) *versus* $d_{N-H...O}$ relationship[22,23] can be described with the following equation

$$v = v_0 + v_1 \exp(d/d_0) \quad (1)$$

Where $v_0 = 0.23089$ nm, $v_1 = 0.00674$ nm and $d_0 = 1475.32977$ cm^{-1}

The calculated N...O distance is then equal to 0.2935 nm. Consequently, at RT the hydrogen bonding cannot have any significant effect on the silk conformation, in contradiction with many assertions in the literature. In the case of *Nephila* spider silk, the band detected at 3224 cm^{-1} involves a shorter N...O distance, ~0.285 nm.[22–24] Such a distance remains too large to determinate the macromolecule conformation but can explain the small bathochromic shift of the water band (3395 cm^{-1} in *Nephila vs* 3430 cm^{-1} in *B. mori* silks).

Figure 5(a) compares the amide A region for the different types of fibre.[19] The spectra have been normalized based on the νC–H massif at 2932 cm^{-1}. The positions of the Gaussian band at 3325 and 3465 cm^{-1} were fixed during fitting. The areas of each component are compared in Fig. 5(b). The difference in the relative areas of the different components is related to the difference in microstructure order at the short scale.[19] It shows that types I and IV are rather similar in microstructure: both of them have 'crystalline'/amorphous ratios more than 1, but Type I is more amorphous while Type IV is more crystalline. Taking into account the mechanical property, both types I and IV exhibit the high value of ultimate stress/strain. Type I shows the highest Young's modulus. Type II has the strongest amorphous component and Type III contains the highest level of water. The analysis at the fracture tip of broken fibre shows marked modifications for Type

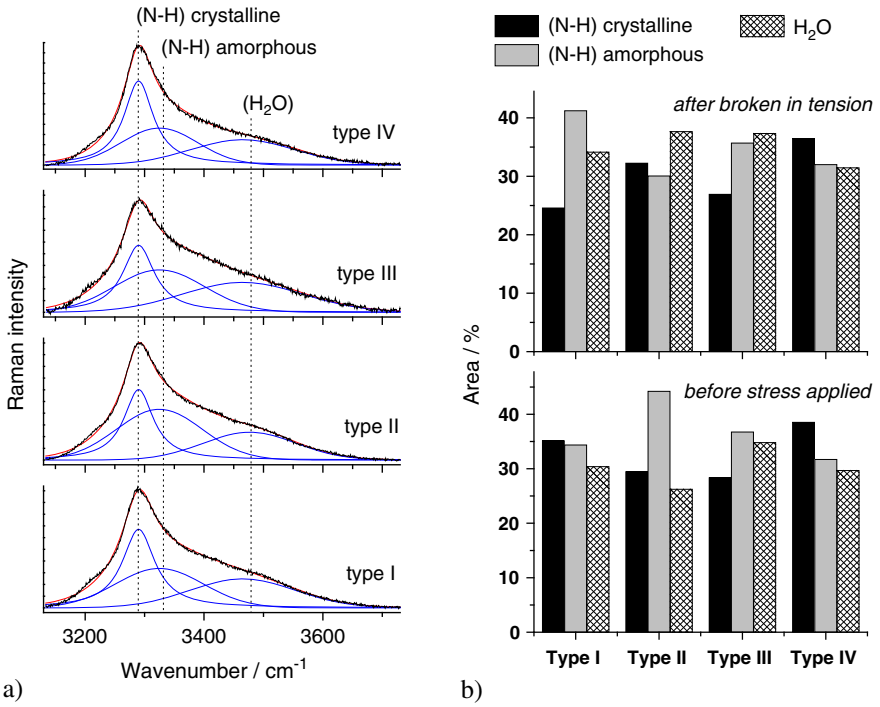

Figure 5. (a) Representative Raman spectra measured before tensile testing for type classified according to Fig. 1(b) areas of the different components are compared and measured before and after failure. Five fibres have been measured for each type a few days after the fracture.

Journal of RAMAN SPECTROSCOPY

I (fresh fibre) and Type II (the most amorphous) fibres. Residual stress has been previously revealed in broken PA66 fibres.[24] A more detailed statistical approach is mandatory to further the understanding of the modifications of the fibre at the fracture tip.

*ν*N–H wavenumber shift *vs* controlled strain: creep behaviour and procedure definition

Figure 6 shows the dependence of the νN–H on the strain of the water saturated fibres. The recording times were rather long (Table S1) and the fibres broke close to the laser spot location much earlier than without laser illumination. Consequently, tests on many fibres were needed to explore the whole tensile behaviour, from the elastic regime to the highest levels of strain. For instance, if samples 0 and 5b were measured at more than 3 controlled strains, the others were only possible at 2 or 3 data points, but there is significant step of wavenumber with the 0 and 5b curves. For the curve 0, when the strain increases from 4% to 6% the wavenumber makes a marked step up. Looking at Table S1, the measurement at 4% strain was made overnight, over 12 h. A similar singularity is observed with sample 5b when the strain increases from 4 to 5% (overnight 4% stretching). Thus, the wavenumber step corresponds to the slow creep behaviour of the fibre, according to the variation of the component area evidenced in Fig. 5. Note that because the measurement takes many hours, there is a decrease of the load applied (see download segments in Fig. 3).

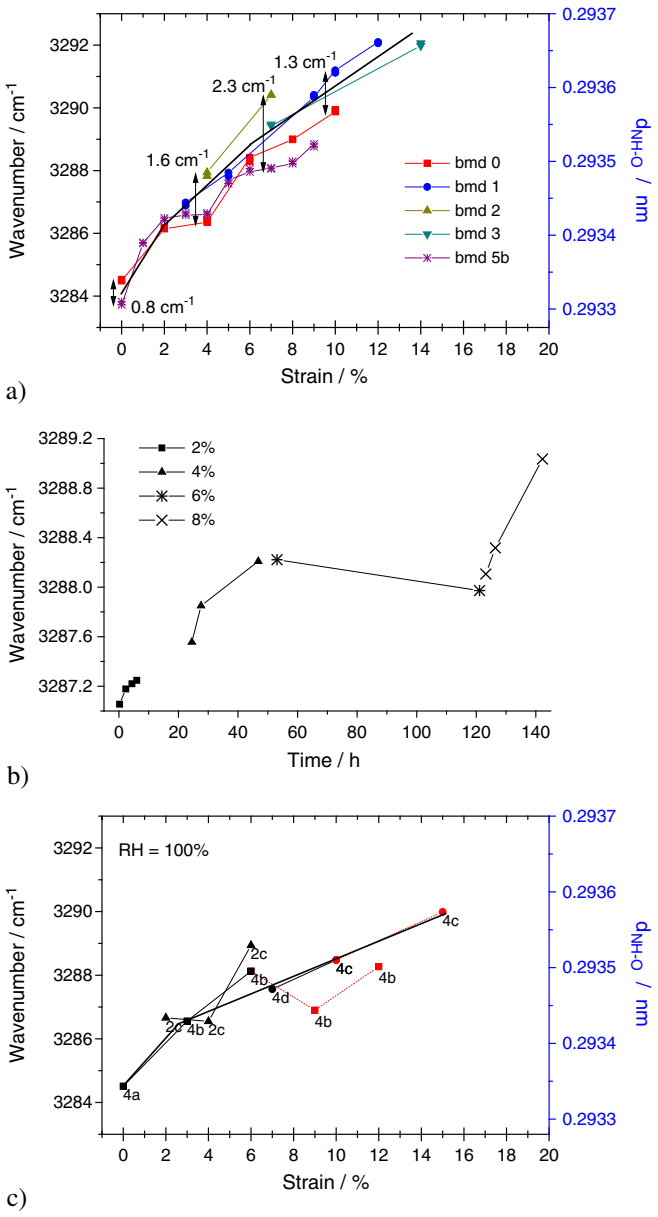

Figure 6. (a) Plots of the νN–H 'crystalline' component wavenumber at different controlled strain levels for a Type III behaviour of water exposed fibres. N–H. . .O distances calculated using the relationship (Eqn 1, see text) are given on the right side axis. The fibres are analysed at room condition (22 °C, 60% RH; see Table S1 for labelling details); (b) the dependence of νN–H wavenumber on stretching time for a fibre at different controlled strains (see Table S2 for details); and (c) plot at different controlled strains for degummed *Bm* fibre saturated with water.

To study the creep behaviour of silk fibres, spectra were measured under the same conditions (recording time = 1800 s, 2 accumulations) after the fibre had been strained to a certain point. Five different lengths of the same fibre were studied, but most of them were analysed only at less than three positions because of a failure. At least, there was one sample that could be measured at 2, 4, 6 and 8% over a week (Table S2, Figs 6(b) and (c)). All received spectra were treated and fitted with the same conditions as described above. The observed wavenumber shift is ~0.1 cm^{-1} h^{-1} except during the yield regime where it is almost equal to 0. This particular behaviour results from the transition taking place beyond 4% of strain with the lengthening of the helix (α−β transition). A very similar feature has been observed for keratin fibres.[8] Considering the time then used to make a measurement (1800 s, 4 accumulations), the variation occurred with a stretching time was similar to the XY spectrometer resolution/accuracy (~0.1 cm^{-1}).

Degummed *B. mori* fibre saturated with water

Raman analysis under controlled strain for a sample takes usually a week. A fibre saturated with water could be used for 1 or 2 measurements before it dried significantly. Therefore, a wide mouth plastic pot containing water was placed beneath the fibre, which was in contact with the water. The fibre was soaked by the water raised by the water meniscus (Fig. 2). The fibre was first soaked in water for 24 h. After each day of measurement (two runs) the fibre was soaked again for 3 h. Raman spectra of water saturated fibre exhibited a high level of background noise.[13] A small 1750 cm^{-1} band, indicating C = O branches interacting with water was often detected. Baseline subtraction and noise filtration were necessary before curve fitting. Results are shown in Fig. 6 (c). Note the rather strong strain dependence below 3–4% of strain and then a lesser one as observed in the case of macroscopic behaviour (Type III, Fig. 1).

Hand spun fresh *B. mori* fibre

Very fresh silk fibres spun by hand from a mature larva exhibited mostly Type I behaviour.[19] As reported before, a series of samples were prepared from the same fibre, identified by the letters of the alphabet and then extreme samples of the series mechanically tested (Fig. 3(a)). After baseline subtraction, noise filtration and fitting the results are plotted in Fig. 7(a): the wavenumber increases strongly with strain below 4%, but from 6% up to the fracture it varies along a quasi plateau, as observed macroscopically in Fig. 1.

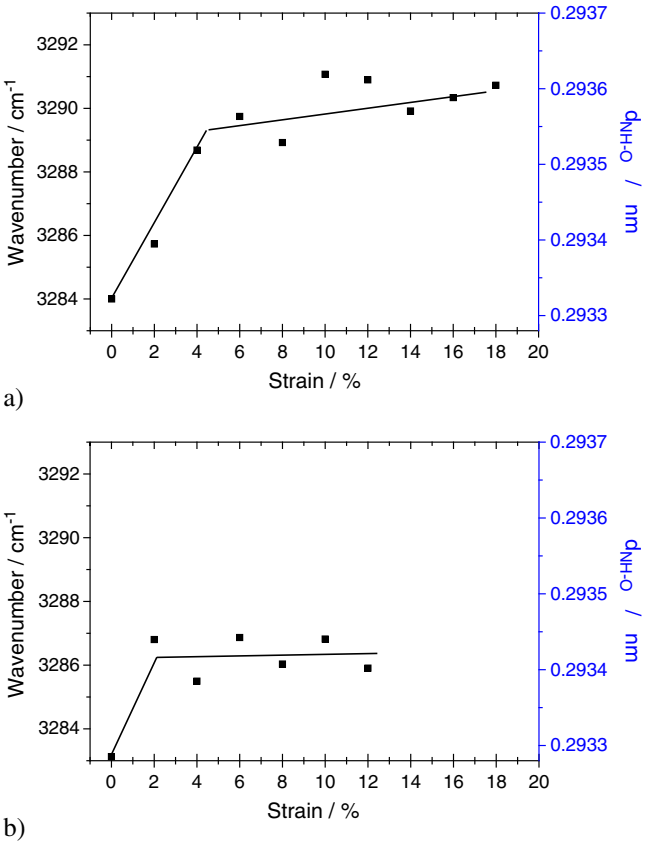

Figure 7. Plot of the νN–H 'crystalline' component wavenumber at different controlled strain levels of a Type I (a) behaviour *Bm* and Type IV *Nephila* (b) fibre. N–H. . .O distance calculated using relationship are given on the right side axis.

Type IV *Nephila* fibre

Figure 7(b) shows the results obtained with dried *Nephila* fibre. The corresponding mechanical behaviour is given in Fig. 3(b). After treatment and fitting, the wavenumber of the strongest component is plotted. A very clear plateau is observed above 2% of strain.

Macro/nano relationship

Figure 8 compares the results of silk fibres, which were characteristic for the four mechanical behaviours with the same Raman shift scale. A good correspondence is obvious with the macroscopic behaviour of Fig.1. Types I and IV exhibit a clear plateau reflecting their 'better' crystallinity. Consequently, the extension jump of the macromolecule (because of the helix opening at the α–β transition) is more efficient. On the other hand, types II and III exhibit a smooth transition around 4–6% of strain and no plateau. Except for the Type III fibre for which the initial Young's modulus is significantly inferior (as observed macroscopically), at the chemical scale there is not a significant difference from the other Types. It is obvious that the water insertion modifies the macromolecule conformation/structure and hence the mechanical behaviour.

Conclusion

The analysis of Raman spectra under controlled strain was made for the different types of silk selected for their distinctive

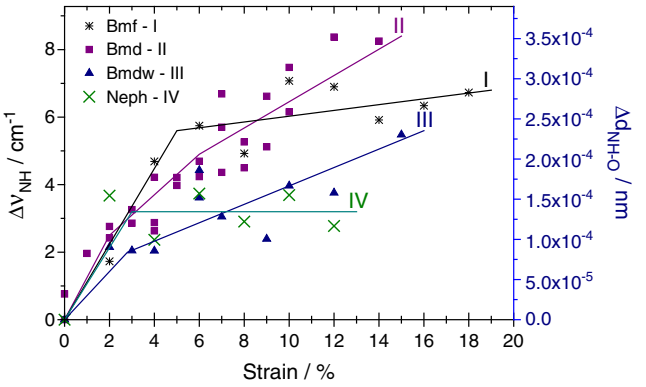

Figure 8. Comparison of the different νN–H wavenumber shifts *versus* controlled tensile strains for types I to IV behaviour.

tensile stress–strain behaviours. The νN–H mode was used because the strong anharmonicity of the hydrogen bond gives rise to a larger wavenumber shift *versus* mechanical perturbation. The nature of hydrogen bonding makes the N–H wavenumber very sensitive to change in the geometry of neighbouring acceptors. The macroscopic elastic (Hookean) regime is also the elastic regime at the bond scale. The threshold between the elastic regime and the quasi-plateau because of the α (helix)-β (sheet) transition is well observed for Type I and Type IV behaviours, as are those of the most ordered materials on the basis of the area of the νN–H component assigned to the vibrators in the nonamorphous regions. As observed at the macroscopic level, the behaviours of types II and III are different, showing no clear-cut transition. The measurement of the νN–H bandwidth at low temperature (10 K, e.g. free of any dynamic broadening), is three times that measured at RT for PA66 synthetic polyamide fibres and confirms the high static disorder of silk macromolecules.

The long recording time required to obtain valuable spectra in the studied wavenumber range leads to a significant relaxation (creep) and associated structure change. Although this last difficulty limits the statistical confidence, the reproducibility is good. The bond length variation calculated from Eqn (1) (~0.0003) is much smaller than the strain (10% of 0.285 nm = 0.0285 nm), i.e. ~1%) as expected for a side-backbone bond (N–H) that is not directly stretched by the fibre tension.

Acknowledgements

Dr Bernard Mauchamp (INRA) is kindly acknowledged for the silk samples and for many discussions. Thanks to Dr Anthony Bunsell for many advices regarding the mechanical analysis and the critical reading of the manuscript and to Drs A. Percot and A. Slodczyk for their help in recording helium temperature spectra. This work was partly supported by ANR NANOSOIE and the project 'National Foundation for Science and Technology Development, Vietnam'.

Supporting information

Supporting information may be found in the online version of this article.

Journal of RAMAN SPECTROSCOPY

References

[1] C. Vepari, D. L. Kaplan, *Progr. Polym. Sci.-Polym. Biomedical Appl.* **2007**, *32*, 991.
[2] D. A. Tirrell, M. J. Fournier, T. L. Mason, *Curr. Opin. Struct. Biol.* **1991**, *1*, 638.
[3] H. Heslot, *Biochimie*, **1998**, *80*, 19.
[4] Y. Liu, X. Chen, J. Quian, H. Liu, Z. Shao, J. Deng, T. Yu, *Appl. Biochem. Biotech.* **1997**, *62*, 105.
[5] V. Jauzein, Ph. Colomban, in A. R. Bunsell, P. Schwartz (Eds.), Handbook of Tensile Properties of Textile and Technical Fibres, CRC Woodhead Publishing Ltd, Oxford, **2009**, pp 144–178.
[6] A. Marcellan, Ph. Colomban, A. Bunsell, *J. Raman Spectrosc.* **2004**, *35*, 308.
[7] Ph. Colomban, J. M. Herrera Ramirez, R. Paquin, A. Marcellan, A. Bunsell, *Eng. Fract. Mech.* **2006**, *73*, 2463.
[8] R. Paquin, Ph. Colomban, *J. Raman Spectrosc.* **2007**, *38*, 504.
[9] Ph. Colomban, G. Gouadec, *Comp. Sci. Tech.* **2009**, *69*, 10.
[10] Ph. Colomban, *Comp. Sci. Tech.* **2009**, *69*, 1437.
[11] J. Sirichaisit, R. J. Young, F. Vollrath, *Polymer* **2000**, *41*, 1223.
[12] Ph. Colomban, G. Sagon, M. Lesage, J. M. Herrera Ramirez, *Vib. Spectrosc.* **2005**, *37*, 83.
[13] Ph. Colomban, H. M. Dinh, J. Riand, L. C. Prinsloo, B. Mauchamp, *J. Raman Spectrosc.* **2008**, *39*, 1749.
[14] T. Lefèvre, F. Paquet-Mercier, S. Lesage, M. E. Rousseau, S. Bidard, M. Pezolet, *Recent Progr. Vib. Spectrosc.* **2009**, *51*, 136.
[15] Ph. Colomban, *Adv. Eng. Mater.* **2002**, *4*, 535.
[16] Ph. Colomban, *Ceram. Trans.* **2000**, *103*, 517.
[17] H. M. Dinh, C. Paris, Ph. Colomban, B. Mauchamp, Comptes-Rendus JNC 16, 16èmes journées nationales sur les composites, Toulouse, Ph. Olivier & J. Lamon Eds, AMAC: Paris, **2009**. http://hal.archives-ouvertes.fr/docs/00/39/75/75/PDF/244b.pdf
[18] H. M. Dinh, H. El Baghli, Ph. Colomban, Proc. APCTP-ASEAN Workshop on Advanced Materials Science and Nanotechnology-AMSN 2008: Nha Trang (Vietnam) September 15th-21th, **2008**.
[19] Ph. Colomban, H. M. Dinh, A. R. Bunsell, B. Mauchamp, *J. Raman Spectrosc.* **2012**, DOI: 10.1002/jrs.3122.
[20] H. M. Dinh, Raman/IR study of the variability of proteic fibres: relationship between local structure, treatments and (nano)mechanical properties of silk fibres and films, Université-Pierre-et-Marie-Curie (UPMC Paris 6) PhD thesis: Paris, **2010**. http://www.ladir.cnrs.fr/pages/colomban/Manh-Thesis.pdf
[21] G. Gouadec, Ph. Colomban, *Progr. Cryst. Growth Charact. Mater.* **2007**, *53*, 1.
[22] A. Novak, *Struct. Bond.* **1974**, *18*, 177.
[23] Ph. Colomban, A. Gruger, A. Novak, A. Regis, *J. Mol. Struct.* **1994**, *317*, 261.
[24] J. M. Herrera Ramirez, Ph. Colomban, A. Bunsell, *J. Raman Spectrosc.* **2004**, *35*, 1063.

